

State of the art in digitization of historical maps and analysis of their metric content

*Original*

State of the art in digitization of historical maps and analysis of their metric content / Roggero, Marco; Soleti, Anna. - In: TERRITORIO ITALIA. - ISSN 2240-7707. - STAMPA. - 2015:1(2015), pp. 33-50. [10.14609/Ti\_1\_15\_3e]

*Availability:*

This version is available at: 11583/2616675 since: 2015-09-08T13:11:54Z

*Publisher:*

Agenzia del Territorio

*Published*

DOI:10.14609/Ti\_1\_15\_3e

*Terms of use:*

This article is made available under terms and conditions as specified in the corresponding bibliographic description in the repository

*Publisher copyright*

(Article begins on next page)

\* Marco Roggero

\*\* Anna Soleti

# State of the art in digitization of historical maps and analysis of their metric content

DOI: 10.14609/Ti\_1\_15\_3e

**Keywords:** Historical cartography, digitization, photogrammetry, georeferencing.

**Abstract** The present work discuss the digitization and georeferencing of the cartographic heritage preserved in the public archives, with special attention to image quality, support deformation analysis and metric content verification. The use of the photogrammetric techniques is suggested, with some applications to the Sabaudian cadastre.

## INTRODUCTION

The cartographic heritage preserved in the public archives is considerable, but often is very difficult to access it. The management state of many public archives is dramatic. Not always the archives, especially at local agencies, have an inventory, or rooms suitable for document preservation and consultation. Maps are often stored rolled up, resulting in deformation of the paper, or bounded in atlases for which it is impossible to scan them or the photographic reproduction without distortion. The binding also often hides part of the map. The paper is not only distorted, but often fragile, making it difficult both the consultation that digitization.

Many technical options are possible for historical maps digitization, the classical photographic reproduction, scanning or photogrammetric reproduction. In all cases the first aspect to consider is the quality of the photographic image, which is not always handled with the necessary care. For this we will face some photographic issues of fundamental importance in the photogrammetric acquisition but also in the simple documents digitization.

In old maps the geometric properties of the content cannot be distinguished from the alteration of the material, but when the paper support is in good conditions and can be considered non deformed we are able to investigate their metric content. However the deformation of the support is not negligible in many cases and we will discuss how it can be determined through photogrammetric techniques.

\* Researcher - Politecnico di Torino, Dipartimento di Architettura e Design, [marco.roggero@polito.it](mailto:marco.roggero@polito.it)

\*\* Architect, [soleanna70@gmail.com](mailto:soleanna70@gmail.com)

Georeferencing is a fundamental task in the study of historical cartographic heritage and make it possible to compare an old map with a recent map or an ortophoto. The availability of Ground Control Points measured by GNSS is useful both for georeferencing that for the verification of the metric content of the map. An example of map georeferencing and mosaicking is discussed, using some maps of the Sabaudian cadastre, and their metric content has been verified finding unexpected accuracy.

## PHOTOGRAPHIC ASPECTS

Due to the required accuracy in historical maps reproduction, it is necessary to take in account for several photographic aspects, related both to geometric and to radiometric quality of the images. The main geometric deformation, the radial distortion, can be automatically handled in the photogrammetric images orientation process. Automatic camera calibration via self-calibration is now the norm in close-range photogrammetry. This is irrespective of whether the cameras to be calibrated are high-end metric, or the digital SLRs and consumer-grade models that are increasingly being employed for image-based 3D measurement. Automation has greatly simplified the calibration task, but there are real prospects that important camera calibration issues may be overlooked in what has become an almost black-box operation.

We must note that modern SLR camera and software can automatically correct the radial distortion. In this case the self-calibration will estimate residual distortions.

Camera calibration parameters, and especially those related to lens distortion, vary significantly with zoom and focus setting. Even using a fixed focus lens, the effect of focusing cannot be neglected in close-range photogrammetry and this is one of the reasons for which in this case the self-calibration is preferable to the use of constant calibration parameters. Mathematical models have been formulated to describe the variation of radial lens distortion with focus [Brown, 1971] and there has been a recent development, called zoom-dependent (Z-D) calibration [Fraser & Al Ajlouni, 2006] which models the variation of lens distortion with zoom setting, thus removing the necessity for the camera zoom setting to be fixed and stable during the image capture process. Nevertheless, recording images with a fixed zoom and focus setting remains the universal practice within close-range photogrammetry. There may well be more than a single zoom/focus setting employed in a single image network, but there needs to be a calibration for each setting, or a geometric arrangement that supports the simultaneous self-calibration for all settings.

In terms of achievable accuracy with automatic camera self-calibration, RMSE values of around 0.05 to 0.1 pixels can be generally anticipated for digital SLR cameras with fixed focal length lenses, whereas 0.1 – 0.3 pixels is more representative for less expensive cameras with integrated zoom lenses. Such calibration accuracy is certainly adequate for a host of measurement applications. While it is recognized that monochrome digital cameras have accuracy advantages over color cameras, all consumer-grade through to professional digital cameras nowadays incorporate color filter arrays whereby only one color is recorded at each pixel location. Most commonly it will be red, green or blue as a consequence of the widely used Bayer Pattern filter array. There are basically three factors limiting photogrammetric accuracy of color cameras, as compared to their Black and White equivalents. The first is the interpolation of the Bayer Pattern required to produce full RGB colors for each pixel, and thus an inherent loss of spatial resolution of the sensor. The second factor is the metric impact of the in-camera pre-processing that is carried to convert a 10-, 12-, 14- or 16-bit recorded RAW image to a more common 8-bit format such as JPEG. The third is chromatic aberration.

Chromatic aberration is a type of distortion in which the colors does not focus to the same convergence point. It occurs because lenses have different refractive indices for different wavelengths of light (the dispersion of the lens). The effect of chromatic aberration can be seen when examining a zoomed-in section of a color image, especially in high contrast areas. The image manifests color fringes, mainly in the radial direction, with the 'red-ish' pixels smeared in the opposite direction to 'blue-ish' pixels, and the 'green-ish' pixels left in focus at the centre of the fringe (in the typical case where the lens is set for optimal focus of green light). The effect becomes more pronounced with increasing radial distance. Since the focal length of a lens is dependent on the refractive index, different wavelengths of light will be focused on different positions.

There are two types of chromatic aberration: axial (longitudinal), and transverse (lateral). Axial aberration occurs when different wavelengths of light are focused at different distances from the lens, *i.e.*, different points on the optical axis (focus shift). Transverse aberration occurs when different wavelengths are focused at different positions in the focal plane (because the magnification and/or distortion of the lens also varies with wavelength).

In term of calibration parameters, due to chromatic aberration each color channel will have a distinct principal distance and radial lens distortion profile, even if the effect of chromatic aberration is generally acknowledged but not specifically accounted for in camera calibration. The presence of variations between principal distance and radial lens distortion coefficient values for the R, G and B channels constitutes a possible source of error for camera self-calibration. Chromatic aberration is inversely proportional to the focal length so is particularly important in wide-angle lenses. It can be minimized by using an achromatic lens, in which materials with differing dispersion are assembled together to form a compound lens. The most common type is an achromatic doublet, with elements made of crown and flint glass. A very practical (but not cheap) means to minimize the metric impact is to seek out a lens which displays very little chromatic aberration. Chromatic aberration minimization via software requires access to the raw camera image, which contains the original and separate R, G and B information.

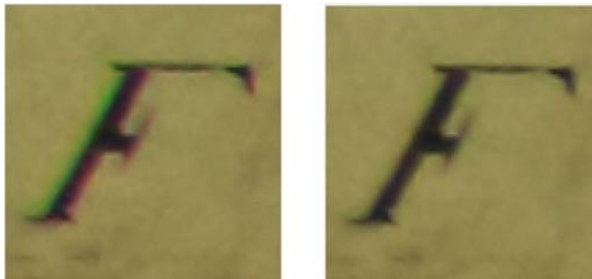


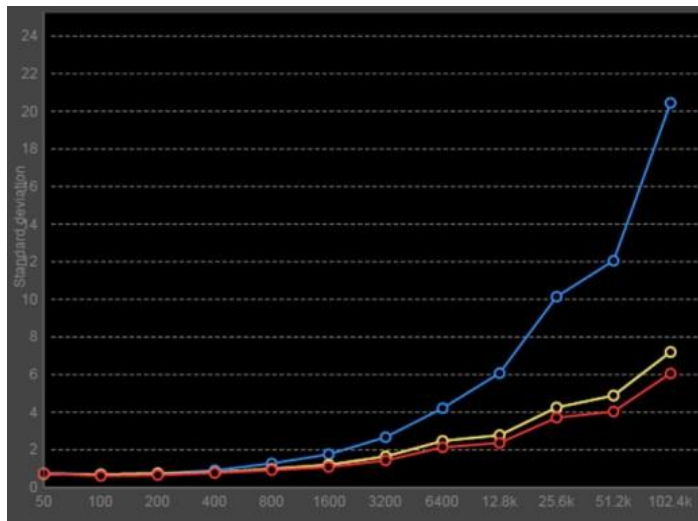
**Figure 1** Chromatic aberration correction on raw Canon CR2 image, via Digital Photo Professional software

Also vignetting, the reduction of brightness and saturation at the image periphery, can be corrected in raw images; this is particularly important in image blending to create image mosaics and textures.

The camera used in the present work is a Canon EOS 5D mark III, equipped with fixed focus lenses:

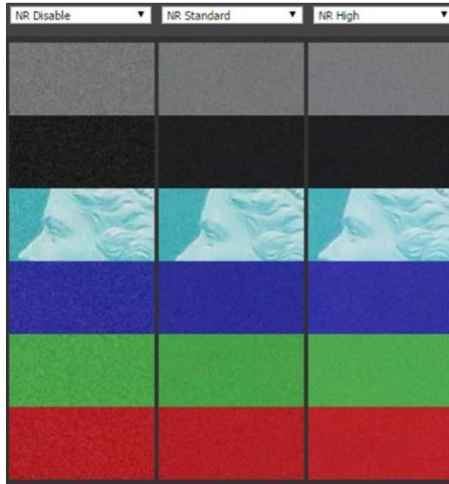
- Canon EF 14 mm f/2.8L II USM
- Canon EF 50 mm f/2.5 compact macro

Image acquisition has been performed using two white light photographic studio lamps. In order to obtain fully focused images the diaphragm must be closed extending enough the depth of field. The use of tripod can be avoided by using lighting and a good ISO sensitivity, in order to obtain quite short exposures. The choice of ISO is always a compromise between sensor sensitivity and image noise. To evaluate the acceptable level of noise is possible to use the online instrument available at Digital Photography Review. Examining the Canon EOS 5D Mark III's measured noise standard deviation at different ISO e with different noise reduction settings, we can see that the noise level remains on the same level up to 1600 ISO also without noise reduction (Figure 2). Of course this can only be achieved by increasing noise reduction as you increase sensitivity. There is practically no benefit to switching noise reduction off at low ISOs, and a difference between the 'Off' and 'Standard' settings only becomes visible at ISO 1600.



**Figure 2** Canon EOS 5D mark III ISO vs. noise standard  
(● NR disabled, ● NR standard, ● NR high)

As shown in previous figure, the effect of noise reduction algorithms became visible at higher ISO. For example at 6400 ISO we can appreciate the effect of noise reduction, even if there are small differences between standard and high NR level (Figure 3).



**Figure 3** Canon EOS 5D mark III: effect of noise reduction at 6400 ISO

At higher ISOs the NR 'Off' settings gives you some additional fine detail over the 'Standard' and higher settings but at very high ISOs, 25600 and above, the 'Standard' setting is the better options, as otherwise the noise levels are too intrusive. Overall the Canon EOS 5D Mark III achieves very low levels of measured noise across the ISO range but this is paid for with a loss of fine detail at higher sensitivities. The two extended settings, ISO 51200 and 102400 should be reserved for emergency situations only, but up to ISO 25600 the camera's JPEGs are usable at least at smaller output sizes. The acquisitions with the Canon EF 14 mm f/2.8L II USM have been performed using a diaphragm f/8.0, exposure 1/100 s at 1000 ISO.



**Figure 4** Image sample acquired by Canon EOS 5D mark III with Canon EF 14 mm f/2.8L II USM, f/8.0, 1/100s, 1000 ISO

Image pre-processing includes chromatic aberration, vignetting corrections and the conversion of raw CR2 files in JPG or TIFF format.

**DISTANCE MEASUREMENT ON HISTORICAL CADASTRES**

Distances can be measured on the map by using a protractor compass. To measure distance with the accuracy of the graphicism error, the graphic transverse scale is used, also called Tychonic scale from the name of the astronomer Tycho Brahe (1536-1601).

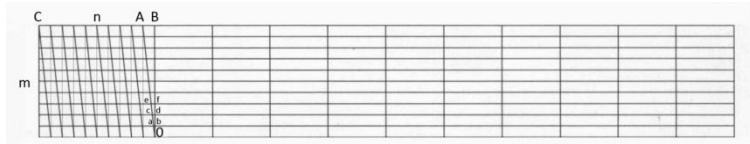


**Figure 5** Construction of the Tychonic scale

To build it choose a base segment CB and carry it different times on a straight base line. From these points draw as many normal segments of equal height. Divide the base CB in *n* equal parts and the normal segment at the left in *m* parts (a common value for both *n* and *m* is 10). Track *m* straight lines parallel to the base line and *n* oblique lines, as shown in the drawing. Because the triangles **Oab**, **Ocd**, **Oef** and **OAB** are similar, it follows that

$$\frac{ab}{AB} = \frac{1}{m} AB, \quad \frac{cd}{AB} = \frac{Od}{OB} = \frac{2}{m}, \quad \frac{ef}{AB} = \frac{Of}{OB} = \frac{3}{m} \dots$$

So

$$ab = \frac{1}{m} AB, \quad cd = \frac{2}{m} AB, \quad ef = \frac{3}{m} AB$$

Because we can  $AB = \frac{CB}{n}$  rearrange the last equations as follows:

$$ab = \frac{CB}{mn}, \quad cd = \frac{2CB}{mn}, \quad ef = \frac{3CB}{mn} \dots$$

The accuracy of the transverse scale is given by

$$\frac{CB}{mn} = ab = t$$

The transverse scale with base CB = 2 cm and *m* = *n* = 10 is called centesimal normal scale, and has an accuracy of *t* = 0.2 mm, equal to the graphicism error.

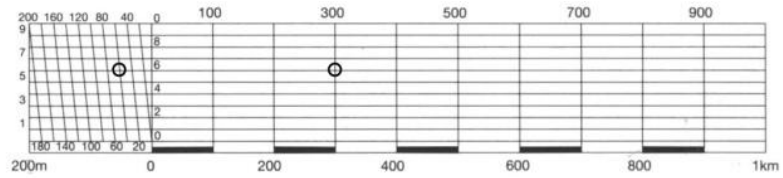


Figure 6 Distance measurement on the Tychonic scale

In the example of Figure 6 we can see how to read a distance on the centesimal normal scale for the nominal scale 1:10000, where the distance between the two points evidenced by the circles is equal to

$$d = 300 + 2 * \frac{CB}{n} + 6 * t$$

$$d = 300 + 2 * \frac{200}{10} + 6 * 2$$

$$d = 300 + 40 + 12 = 352m$$

The general formula for the transverse scale with nominal scale 1:s and base b (in drawing unit) is

$$d = d_1 + s * \frac{b}{n} * \left( c_n + \frac{c_m}{m} \right) =$$

$$= d_1 + c_n * \frac{sb}{n} + c_m * t$$

and it can be easily applied to transverse scales on historical maps, as shown in the example of Figure 7 that refers to a scale of a Sabaudian cadastre.

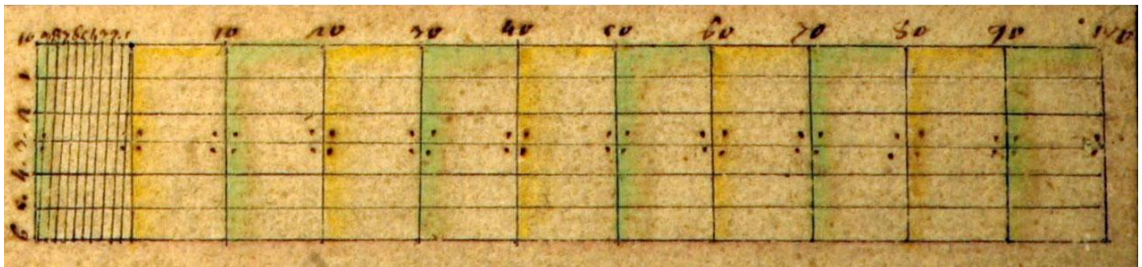


Figure 7 Tychonic scale of a Sabaudian cadastre, with the words "Scala di Trabucchi Centodieci". The scale has been build using the parameters b = 10 trabucchi, m = 6 and n = 10, so its accuracy is 1/6 trabucco or 1 Piedmontese feet, that is equal to 51.4403 cm. Note that the scale construction is inverted respect to the previous example



## MEASURES IN PIEDMONT

The mile of Piedmont is 1/45 of degree in latitude and is equal to 800 *trabucchi*. The *trabucco* is 6 piedmontese feet (*piede*), while 1 *pertica* is 12 feet; one foot is 12 *once* and the distances are represented as *trabucchi:pieci:once*. The length units are resumed in Table .

miglio	2469.136 m	800 trabucchi
pertica	6.173 m	12 piedi
<b>trabucco</b>	<b>3.086 m</b>	<b>6 piedi</b>
<b>piede</b>	<b>0.5144 m</b>	<b>12 once</b>
<b>oncia</b>	<b>0.0429 m</b>	<b>12 punti</b>
punto	0.0036 m	12 atomi
atomo	0.0003 m	

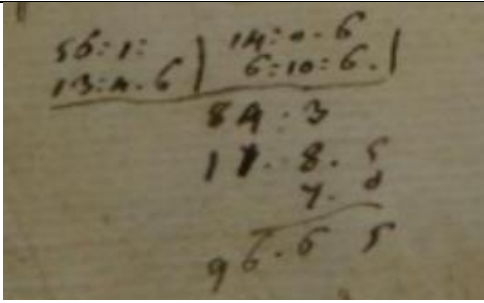


**Table 1** Piedmontese length units and distance representation as *trabucchi:pieci:once*

The surface units are the *tavola*, equal to 1 *pertica*<sup>2</sup> or to 4 *trabucchi*<sup>2</sup> (38.10 m<sup>2</sup>), and the *giornata*, equal to 100 *tavole* (3810.39 m<sup>2</sup>).

## SINGLE IMAGE DIGITIZATION

The most common procedure in historical maps digitization consist in acquiring a single image for each map, that can be enough if the paper support can be considered planar. In this case map digitization requires only three simple steps: remove radial distortion and other aberrations using *a priori* calibration parameters, remove perspective distortion through homography, georeferencing.

To remove radial distortion, vignetting and chromatic aberration we used Canon Digital Photo Professional, but a common and easy solution is to use PTLens software<sup>1</sup>.

Homography transformation is a popular geo-referencing technique based on projective geometry, based on the following equations:

$$X = \frac{ax + by + c}{gx + hy + 1}; \quad Y = \frac{dx + ey + f}{gx + hy + 1} \quad (1)$$

where **x** and **y** are the image coordinates and **X** and **Y** the map coordinates. The main problem in historical maps rectification is to find a sufficient number of ground control points, in order to estimate the 8 unknown parameters **a**, **b**, **c**, **d**, **e**, **f**, **g** and **h**. Because each point generates two equations, a minimum of 4 points is necessary to determine the unknowns, but a certain redundancy is preferable. We suggest a method that uses homography to remove perspective deformation also without ground control points, while by using at least 2 GCPs geo-referencing is possible. More than 2 GCPs are necessary to perform an accuracy assessment of the historical map, and we will show an analysis on a Sabaudian cadastre as example. The method can be used also for mosaicking maps, a task that is necessary managing cadastral maps. If no GCP or very few GCPs are available, it is necessary to

<sup>1</sup> [www.epaperpress.com/ptlens/](http://www.epaperpress.com/ptlens/)

determine the coordinates of a number of points in a local map coordinate system, by measuring a trilateration network on the map. We choose the map points following two simple criteria:

- Some of the points must be on the map boundary and must be common with neighboring maps. This criteria is essential to build a mosaic of neighboring maps.
- Some of the points must be ground control points (minimum 2). The task is not trivial because requires to recognize points on the ground, to be measured by GNSS, or correspondences with a modern map or orthophoto.

For each ground control point was compiled a sheet reporting the place names and the approximate coordinates on the CTR, on the orthophoto and on the historical cadastre, in order to find and measure it by GNSS.

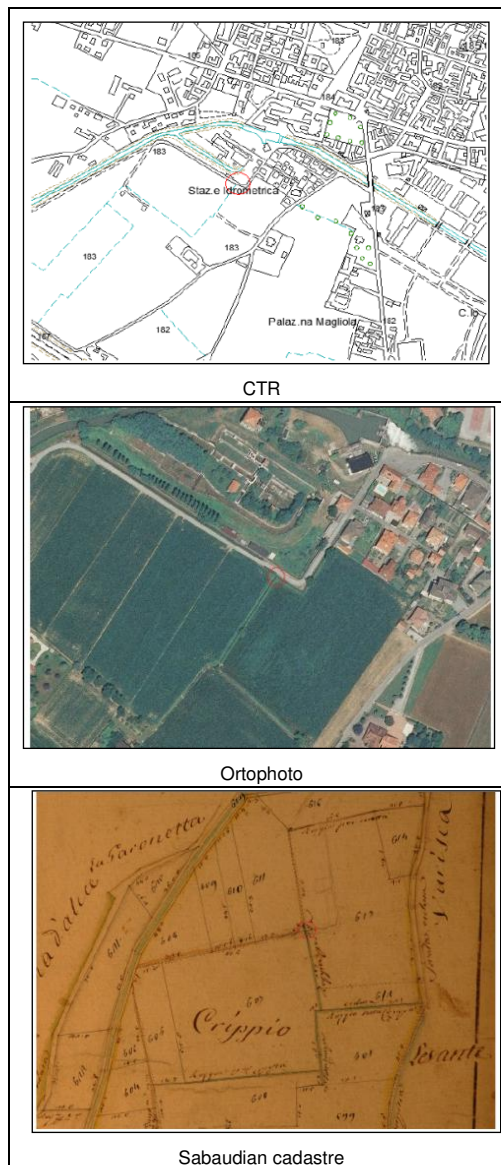


**Figure 8** Individuation of Ground Control Points

Then we connect the points through a trilateration network, that can be optimally and automatically designed by Delaunay criteria. Trilateration edges are measured on the map by protractor compass referring to the tychonic scale and converted in meters. The trilateration of redundant networks is also possible, but requires the measurement of a very high number of distances on the map.

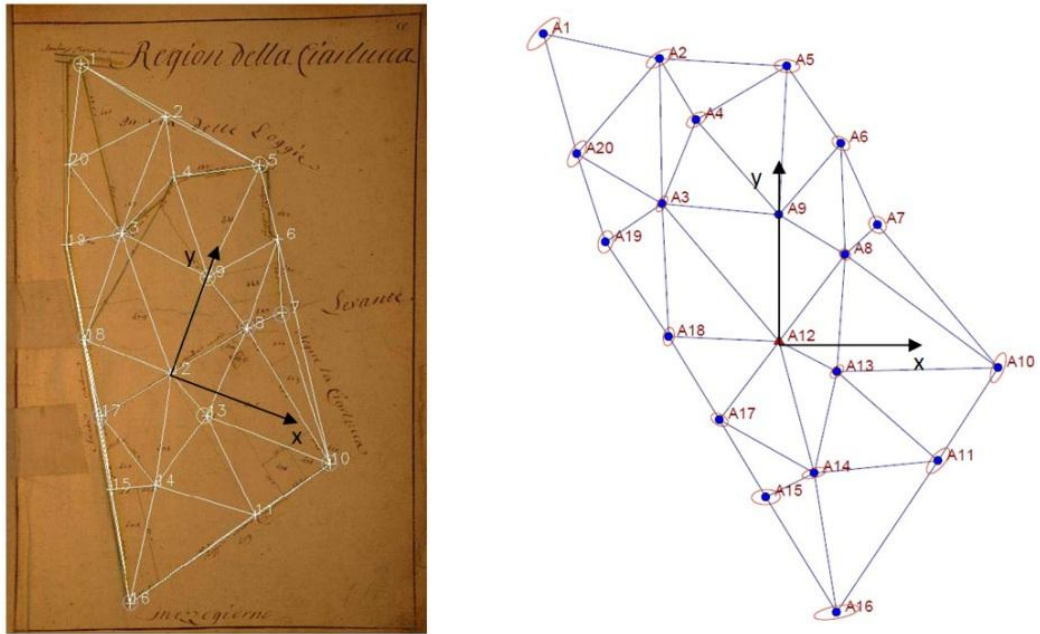


**Figure 9** Trilateration network based on Delaunay criteria. The point A12 has been chosen as origin and A9 as orientation of a local Cartesian coordinate system. Error ellipse of the compensation are represented

One point of the network is chosen as origin and a second point fixed the orientation of a Cartesian coordinate system. The trilateration network is then compensated by least squares in order to obtain local coordinates of the points. In the case that some of the points have known cartographic coordinates, we can compensate a mixed network, where the (pseudo)observations are coordinates and distances. See, as example, the case of the map in Figure 9.

The network scheme has been modified inserting 7 GCPs and some redundant distance measurement, in order to perform data snooping and check the accuracy of the map. The GCPs have been measured on the ground by single frequency GNSS using EGNOS corrections, obtaining coordinates that are accurate at the meter level, that is sufficient for cartographic purposes and the materialization of GCPs.

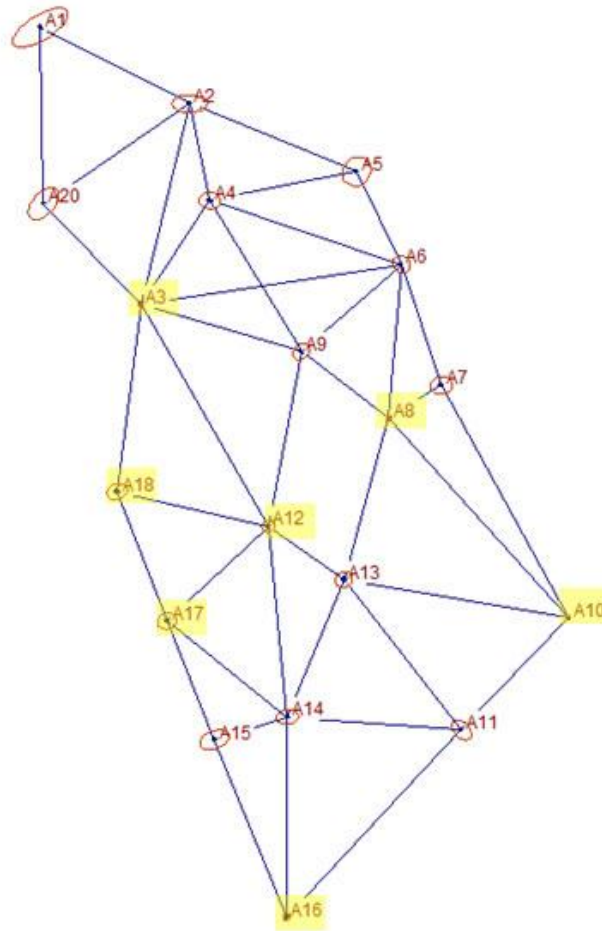


**Figure 10** Mixed network including distances and coordinates of the GCPs (evidenced in yellow)

Network compensation shows a good correspondence of the map with GCPs as well as an excellent internal consistency between the measured distances.

The compensated coordinates with their RMS are reported in Table 2 while a statistic on the residuals of the observed distances after compensation is in Figure 11. Distance standard deviation is about 55 cm or 1 piedmontese feet, equal to the accuracy of the transverse scale on the same cadastral maps.

GCP	E	N	StErr	$\delta_E$	$\delta_N$
A3	433377.540	5024133.615	0.194	0.019	0.005
A8	433660.260	5024003.703	0.181	0.013	-0.044
A10	433865.581	5023775.731	0.186	-0.030	0.045
A12	433523.214	5023880.537	0.840	-0.073	-0.150
A16	433543.792	5023434.345	0.340	0.005	0.018
A17	433407.568	5023772.278	1.453	-0.016	-0.052
A18	433350.537	5023919.738	1.682	0.055	0.004

**Table 2** Compensated coordinates, a priori accuracy (StErr) and horizontal residuals of the GCP ( $\delta_E$ ,  $\delta_N$ ). The standard error refers to the horizontal coordinates obtained by single frequency GNSS and EGNOS corrections. The units are meters.

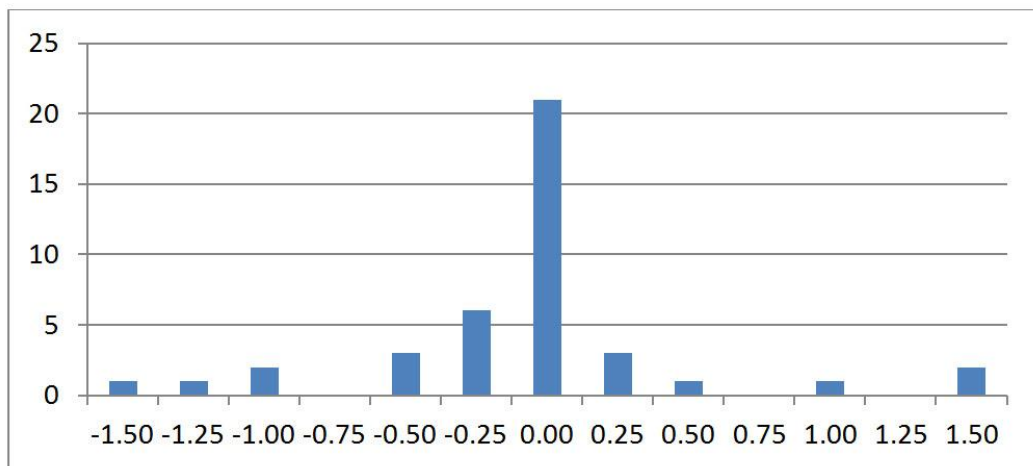


**Figure 11** Observed distances after compensation. Histogram of the residuals. 43 distances have been measured; 2 of them presented residuals larger than 3 m, have been classified as outliers and eliminated. After data snooping the residuals have mean of 0.037 m and a standard deviation of 0.549 m.

The procedure has been applied to 7 neighboring maps of the sabaudian cadastre of Santhià (VC) obtaining a georeferenced mosaic and an exhaustive statistic of its metric accuracy.

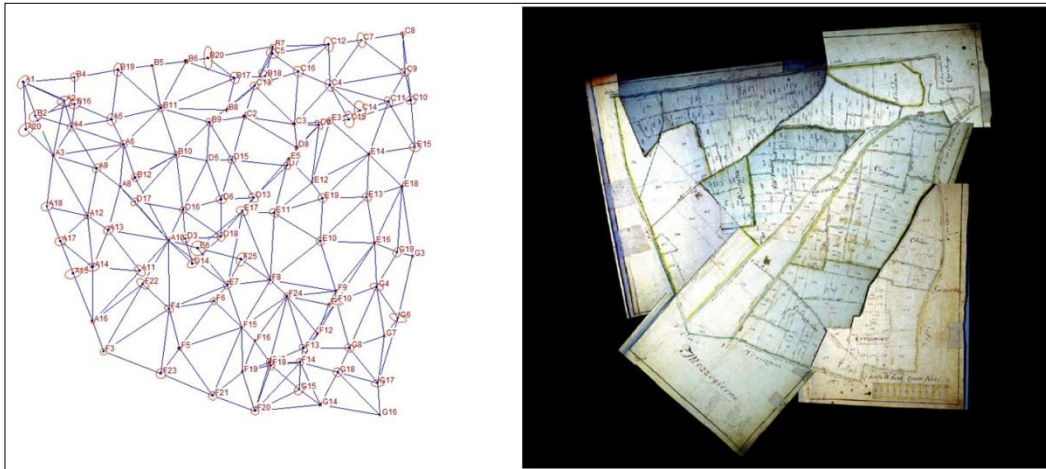


**Figure 12** Compensated complete network, including 306 distances and 40 GCPs, and the georeferenced mosaic of 7 maps of the sabaudian cadastre of Santhià (VC)

## MULTI IMAGE DIGITIZATION

Several studies have been made over the years to obtain a digitization process that could also register in digital shape both the three-dimensional surface of the supporting material (*e.g.* an undulated / deformed map surface) and its two-dimensional high-resolution image. Different solutions have been proposed, based on well consolidated photogrammetric or scanning techniques, to acquire an accurate memory of the map as it was, while the correction of its deformation is a task not completely solved at the state of the art.

The use of triangulation-based laser scanners for the acquisition of three-dimensional data as point clouds, with an uncertainty of about 0.1 mm, has been proposed by Adami *et al.*, 2007. Other applications used static systems for the acquisition of high-resolution stereo images in order to obtain two and three-dimensional products. The system could move along the **X** and **Z** axes, so that they could obtain images with a good overlap and suitable for the 1:1 scale [Tsioukas *et al.*, 2009]. The same research group underlined the value of Structure from Motion software products for the digitization of old maps in atlases and bounded books, in comparison with dedicated book scanning devices [Tsioukas *et al.*, 2012]. The solution proposed in Ballarin, 2014 intends to automate the process of image acquisition, obtaining sequences of oriented images to be processed with Structure from Motion software in a semi-automatic way. The results of the process is a three-dimensional surface that enable to analyze the deformation of the map.

The actual needs, in the contest of public archives, include acquiring three-dimensional data, high-resolution and good operating speed, without complex equipments. The minimum equipment consists of a camera and a pair of lamps to illuminate uniformly the map. It is also possible to use a tripod in case of low illumination.

The suggested operation workflow can be summarized in the following steps:

- Image acquisition
- Image pre-processing
- Image alignment
- Build dense cloud through Structure from Motion
- Build mesh
- Build texture in ortophoto mode
- Gereferencing the texture
- Evaluating map accuracy

While image acquisition and pre-processing follow the same procedures already explained discussing the photographic aspects, image alignment includes automatic self-calibration, that is mandatory to estimate calibration parameters coherent with the focusing conditions during the acquisition, even using fixed focus lenses. As we already pointed out, it is recommendable to maintain a fixed focus by setting manual focusing, and extending the depth of field by closing the diaphragm. However we will have different focusing settings in different acquisition sessions and the calibration parameters must be re-estimated each time. The stability of the calibration parameters can be checked performing different calibration at different focus. We tested the Canon EF 50 mm f/2.5 compact macro in the condition reported in Table 3, acquiring 7 images for each focus distance. In order to obtain fully focused images the diaphragm has been set at f/32 and the sensitivity at 3200 ISO. The estimated focal decreases asymptotically to 50 mm at  $\infty$  focus distance.

Focus distance	c	$x_{pp}$	$y_{pp}$	$k_1$	$k_2$	$k_3$
270	63.4	-0.023	0.342	-4.87E-06	4.30E-08	-9.82E-12
316	60.0	-0.025	0.328	-1.19E-05	4.74E-08	-1.62E-11
400	57.1	-0.037	0.300	-1.76E-05	4.66E-08	-1.53E-11
500	55.2	-0.049	0.330	-2.38E-05	6.04E-08	-3.87E-11
600	54.2	-0.043	0.317	-2.53E-05	5.21E-08	-2.25E-11

The figure is a scatter plot with a grid. The y-axis is labeled 'focal lenght [mm]' and has major ticks at 50,0, 60,0, and 70,0. The x-axis is labeled 'focus distance [mm]' and has major ticks at 0, 500, and 1000. There are five data points plotted as blue circles. The points are approximately at (270, 63.4), (316, 60.0), (400, 57.1), (500, 55.2), and (600, 54.2). A smooth curve is drawn through these points, showing a decreasing trend that levels off towards 50.0 mm as the focus distance increases.

**Table 3** Calibration parameters vs. focus distance. All the unit are in mm

To better understand the potential and critical issues of 3D map digitization, see as example the multi image reconstruction of a cadastral map of Masino dated 1772, conserved in the historical archive of the municipality of Caravino (TO). 11 images have been acquired by Canon EOS 5D mark III, equipped with the Canon EF 14 mm f/2.8L II USM, and then processed by Agisoft PhotoScan<sup>2</sup> in order to obtain the 3D model of the deformed map surface and its ortophoto, that have been scaled using the graphic scale in trabucchi on the map. Observing the model in Figure 13, we can see the nature of the deformations.

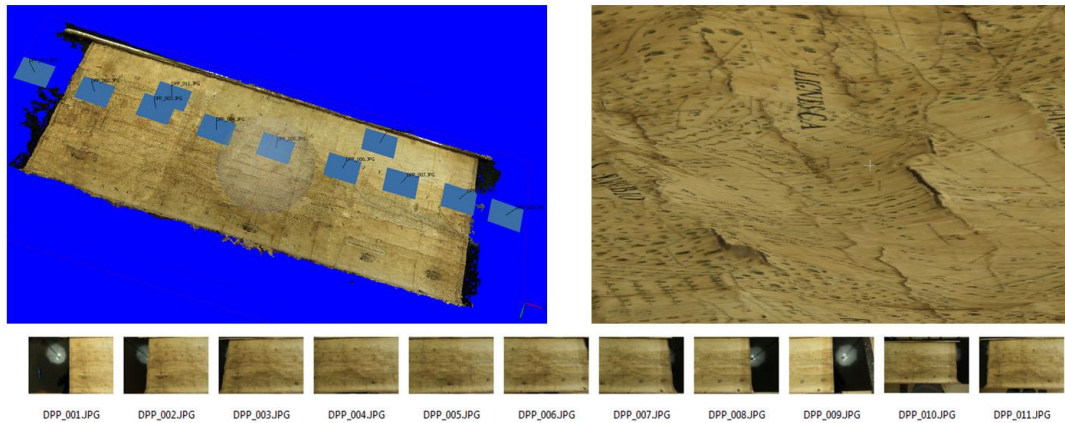


**Figure 13** Images acquired and 3D reconstruction of the cadastral map of Masino, dated 1772. The map has been digitized as it is, and the model shows the deformations of the support

The paper, currently stuck on a canvas, is not well preserved also because the map is kept rolled up and this has caused undulations and breakages. The deformation of the support includes undulations and dilations, that have different effects on the distances measured on the map. Even if the causes of undulation and dilation can be the same (humidity, bending or rolling of sheet) and undulation can also be a consequence of dilation, the effects of dilation are on the plane while the effects of undulation are out of the plane. The effect of dilation is a non uniform variation of the scale factor, that can be recovered by georeferencing using a sufficient number of GCPs. On the other hand the effect of undulation is much more remarkable. We computed the undulation with respect to a mean plane by Cloud Compare<sup>3</sup> (see Figure 14), and we found deviations from the mean plane of the order of 1-2 cm. The effect on the measured distances is a contraction of the order of 1-2 %.

---

<sup>2</sup> [www.agisoft.com](http://www.agisoft.com)

<sup>3</sup> [www.cloudcompare.org](http://www.cloudcompare.org)



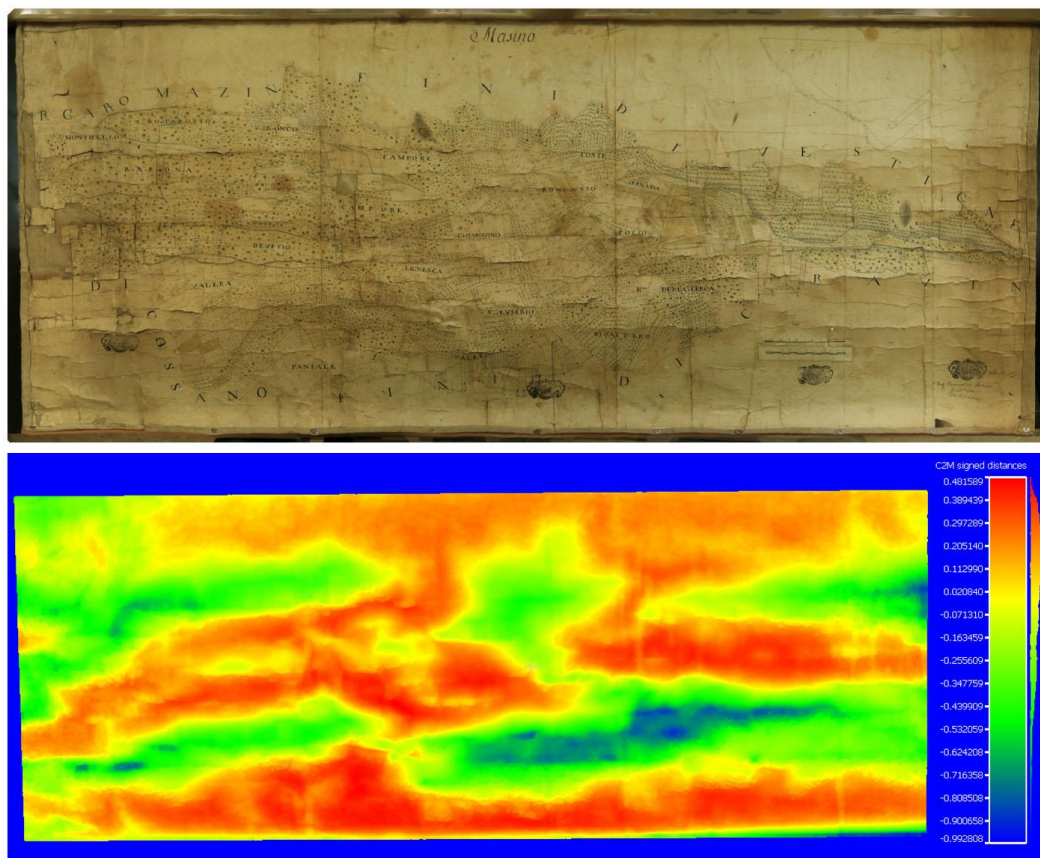


**Figure 14** Orthophoto and DEM of the deformed map. The unit are % of the map width

Georeferencing through triangulation or polynomial wrapping requires a high number of GCP, that is not always easy to find on historical maps. A rough georeferencing can help in this task by overlapping the historical map on a modern cartography or orthophoto. This can be achieved by RST (rotation, scale, translation), fixing the scale factor and the orientation, that requires only two GCP. The orthophoto in Figura 14 has been obtained projecting the 3D textured model on the mean plane and finally georeferenced in ENVI<sup>4</sup> by a polynomial model and 25 GCPs, with a total RMS of 9.4 m. The comparison with a modern cartography in Figura 15 shows a good agreement, even if the RMS on the selected GCPs are quite high. Comparing the results with those obtained on the cadastral maps of Santhià (GCP RMS of about 0.5 m), we can conclude that the deformation of the paper has induced a degradation of the metric content of the map of the order of 10 m on the GCP, although on the map as a whole, the accuracy is worse, since the GCP were chosen in areas where the effect of the deformation was not excessive.

<sup>4</sup> [www.exelisvis.com/ProductsServices/ENVIProducts/ENVI.aspx](http://www.exelisvis.com/ProductsServices/ENVIProducts/ENVI.aspx)

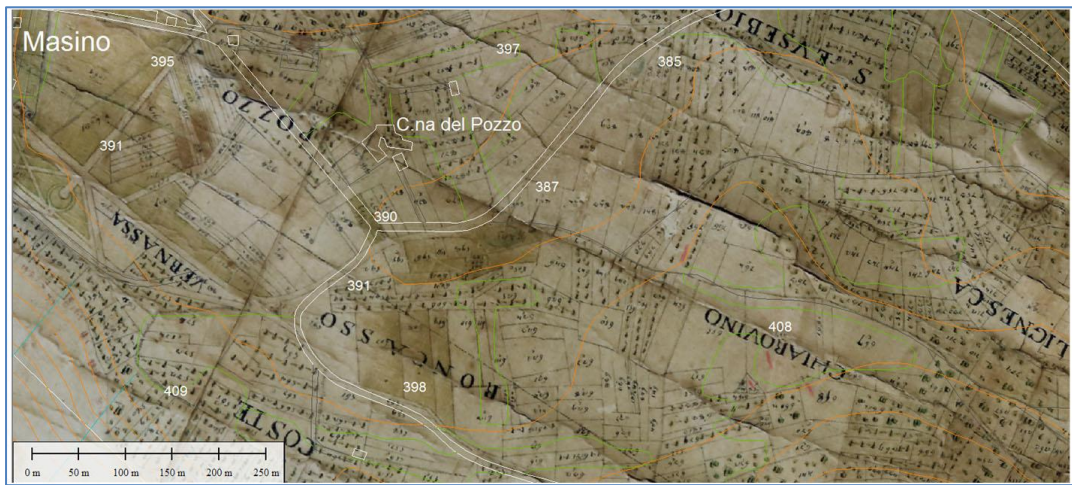


Figure 15 Georeferenced map: superimposition of CTR

## CONCLUSIONS

The analysis carried out on the Sabaudian cadastre show a good cartographic accuracy and demonstrate the effectiveness of the procedures used in surveying in the late XVIII century. It is necessary to remark that the analysis has been conducted on a cultivated and flat area, while the level of accuracy could not be uniform throughout the country and was definitely worse in wooded or mountainous areas. Further analysis are required in areas with different geographical characteristics and are also possible comparisons with other cadastres of the time, including the Napoleonic cadastre that in the same areas of Piedmont was available around 1810, then about 20 years after the Sabaudian cadastre.

From the technical point of view the digitization process it is currently well established, although in practice the procedures proposed here and in the other cited works are not absolutely a standard. The main problem in historical maps digitization and georeferencing remains the paper deformation. While by using a sufficient number of GCPs the paper dilation can be managed, a solution for recovering undulation deformation is not actually available on commercial software and is subject of research. We are working on an algorithm based on the distance measurement on the deformed surface, that seems to be able to recover such deformations almost totally. Automation of the process is also greatly needed, as the heritage of historical maps kept in the public archives is immense, but the main important task, in my opinion, is to build a common and open database of georeferenced maps. This task can be accomplished only by bringing the whole process to a high level of automation, which I think is doable with the exception of the selection of GCPs.

## References

- Adami A., Fregonese L., Guerra F., Livieratos L., Tsioukas V. (2007), Digital Representations And Analysis Of Deformations Induced In Map Supporting Materials. *Proc. of CIPA-2007 International Symposium*. Athens. Greece. Oct. 1-6. 2007
- Brown D.C. (1971), *Close-Range Camera Calibration*. *Photogrammetric Engineering*. 37(8): 855–866.
- Fraser C.S. and Al-Ajlouni S. (2006), Zoom-Dependent Camera Calibration in Close-Range Photogrammetry, *Photogrammetric Engineering & Remote Sensing*. 72(9): 1017-1026.
- Fraser C.S. (2012), *Automatic camera calibration in close-range photogrammetry*, in Proc. Of ASPRS. Sacramento. CA. USA
- Tsioukas V., Koussoulakou A., Pazarli M., Ploutoglou N., Daniil M., Stergiopoulou I. (2012), Scanning or digitizing in libraries? A test on the efficiency of dedicated book-scanning devices in digitizing bound atlases and maps. *e-Perimtron*. Vol. 7. No. 4: 163-169.
- Tsioukas V., Daniil M. (2009), 3D digitization of historical maps. *e-Perimtron*. Vol. 4. No. 1: 45-52.
- Tsioukas V., Daniil M. (2006), Possibilities and problems in close range non-contact 1:1 digitization of antique maps. *e-Perimtron*. Vol. 1. No. 3: 230-238.